# Supporting information for:

## Constructing desired nanofibril network morphology for stretchable polymer films by weakening the intermolecular interaction of conjugated polymer in elastomer matrix and extending the film-forming time

Tao Zhang,[a,b] Yadi Liu,[a,b] Lu Zhang,[a,b] Sichun Wang,[a,b] Junhang Li,[a,b] Jiaming Zuo,[a,b] Xinhong Yu,[a] Qiang Zhang*[a] and Yanchun Han*[a,b]

[a] State Key Laboratory of Polymer Physics and Chemistry, Changchun Institute of Applied Chemistry, Chinese Academy of Sciences, Changchun, 130022, P. R. China

[b] School of Applied Chemistry and Engineering, University of Science and Technology of China, Hefei, 230026, P. R. China

**Materials and Solvents**

N2200 with molecular weight ($M_n$) of 110 kDa and polydispersity index (PDI) of 2.0 was provided by Derthon Optoelectronic Materials Science Technology Co LTD (China). The SEBS that contains 88% (H1221) and 80% (H1052) volume fraction of poly(ethylene-co-butylene) was provided by Asahi Kasei (Japan). PDMS (Sylgard 184) was provided by Dow Corning (America). Trichloro(octadecyl)silane (OTCS) was provided by Sigma-Aldrich (America). 1,2-dichlorobenzene (*o*-DCB), chlorobenzene (CB), and toluene (Tol) were obtained from *J&K* Chemicals (China). The boiling point of *o*-DCB, CB, and Tol are 180.4, 131.7, and 110.6 ℃, respectively.

**Solution and Film Preparation**

For neat N2200 and SEBS solutions preparation, the N2200 and SEBS were firstly dissolved in *o*-DCB, CB, and Tol at 10 mg $mL^{-1}$, respectively. The solutions were then heated at 110 ℃ (*o*-DCB) or 80 ℃ (CB, Tol) for 2 h. For N2200/SEBS blend solutions preparation, the N2200 and SEBS solutions dissolved in the same solvent were mixed with a volume ratio of 3:7 and then heated for 1 h before spin-coating.

For film preparation, the obtained neat and blend solutions were firstly removed from the hot plate. After naturally cooled to room temperature, the solutions were spin-coated at different speed and then annealed at 150 ℃ for 1 h. The thickness of all films was controlled to ~100 nm.

**Mechanical Properties**

The stretched N2200 and N2200/SEBS blend films were prepared by FOE method. The PDMS elastomer used for transfer and stretching stamp was prepared by blending the base and cross-linker in a weight ratio of 10:1 and then cured at 70 ℃ for 10 h. A PDMS slide with the width of 1 cm and

length of 5 cm was cut off and used to stamp the film. After lift the PDMS slide quickly, the polymer layer was delaminated and attached to the PDMS. Subsequently, the film was stretched by using a customized stretching machine. Finally, the stretched film was transferred and laminated to the substrate that modified with a SEBS (H1052) layer. The crack onset strain (COS) of films was determined using an optical microscope (Zeiss Axio Imager A2m). The dichroic ratio of stretched blends was characterized by UV-visible (UV-vis) spectroscopy with a rotational polarizer.

The stress-strain curves of N2200 and N2200/SEBS films were acquired by FOW method. The films were firstly prepared on a silicon substrate that covered with a PEDOT:PSS sacrificial layer. A PDMS with a dog-bone shape was then covered on top of the film and acts as a mask template. The length and the width at the center of the PDMS were 5 and 3 cm, respectively. After oxygen plasma etching treatment for 15 min, a polymer film with dog-bone shape was obtained. And then submerged the substrate into water, the PEDOT:PSS layer dissolves, leaving the film on the water surface. Finally, the floated film was fixed by two PDMS-coated Al grips of a customized stretching machine and stretched at 1 mm $min^{-1}$ until the failure of the film.

**OTFT Fabrication and Characterizations**

The organic field-effect transistors (OFETs) were fabricated in a bottom-gate/top-contact (BGTC) configuration to evaluate the electrical properties of films. Highly *n*-doped silicon wafer with $SiO_2$ (300 nm) was modified by OTCS as reported previously and used as substrate. N2200 and N2200/SEBS solutions were then spin-coated onto it as described in 2.2. Finally, the gold source and drain electrodes (~30 nm, $W$=200 μm, $L$=40 μm) were vacuum-evaporated onto the film. For the stretching devices, FOE method was used to obtain stretched films and SEBS (H1052) was used as dielectric layer. The concentration of the SEBS (H1052) solutions (Tol) used for the fabrication

of dielectric layers for stretched films under single and repeat stretching cycles are 4 and 16 mg $mL^{-1}$, respectively. And these solutions were then spin-coated on the $SiO_2$ at 3000 rpm for 40 s. The electrical measurements of OFET devices was conducted with a semiconductor parameter analyzer (Keysight B1500A). The following equation was used to calculate the field-effect mobility of transistors:

$$I_{D,sat} = \frac{W}{2L} C_i \mu (V_G - V_T)^2 \quad (1)$$

where $I_D$, $W$, $L$, $C_i$, $\mu$, $V_G$, and $V_T$ are the drain-source current, the width of transistor channels, the length of transistor channels, the capacitance, the field-effect mobility, the gate voltage, and threshold voltage, respectively.

**Measurements and Characterizations**

UV-vis absorption spectra of solutions and films and *in situ* UV-vis spectra were measured using the Lambda 750 spectrometer (Perkin-Elmer, Wellesley, MA). The concentration of neat N2200 and N2200/SEBS blend solutions were 0.1 mg $mL^{-1}$.

The atomic force microscopy (AFM) images were acquired from SPA-300HV (Seiko Instruments Inc., Japan). The transmission electron microscopy (TEM) images were acquired from a 100 kV JEM-1011 microscopy (JEOL, Japan).

Out-of-plane grazing incidence X-ray diffraction (GIXRD) was performed on Bruker D8 Discover X-ray thin film diffractometer (Cu-$K\alpha$, $\lambda$ = 1.54 Å). In-plane GIXRD was performed on beamline 1W1A of Beijing Synchrotron Radiation Facility (BSRF, $\lambda$ = 1.54 Å).

Film-depth-dependent light absorption spectroscopy (FLAS) of films was measured by a Diener Zepto Plasma machine. The film surface was etched gradually using oxygen with low pressure and a UV-vis spectrometer (Lambda 750) was used to record the absorption spectra after each etching.

For comparison, the etching rates of neat N2200 and SEBS film are calculated separately by monitoring the changes in film thickness after each etching. The etching pressure, power, and time are 0.4 MPa, 200 W, and 30 seconds, respectively. After each etching, the reduction of neat N2200 and SEBS film thickness is approximately 8.7 and 12.3 nm, respectively. Thus, the etching rate for N2200 and SEBS is 17.4 and 24.6 nm $min^{-1}$, respectively.

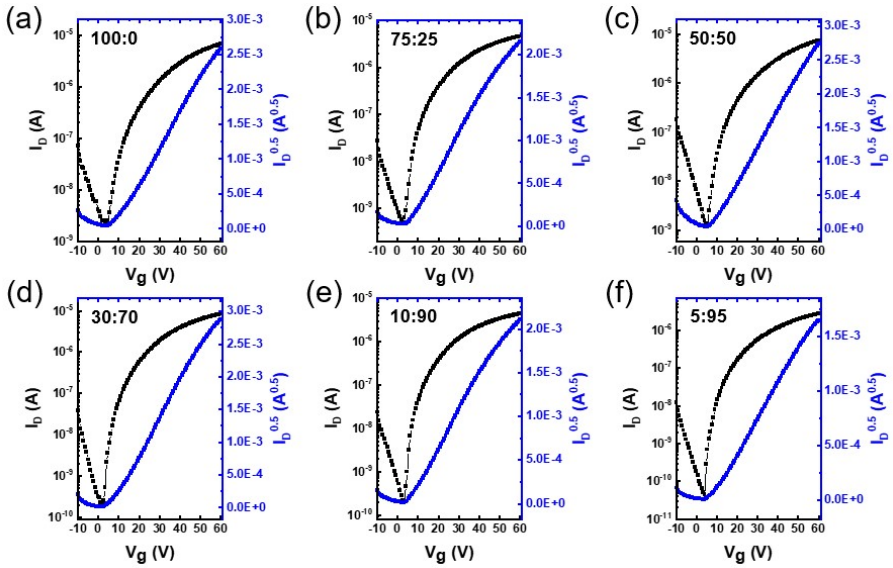


**Figure S1.** Representative transfer at $V_D$ = 60 V of BGTC OFET devices based on N2200/SEBS of different blend ratios, the films are processed by *o*-DCB solvent.

**Table S1.** Corresponding carrier mobility of N2200/SEBS blend films with different blend ratios.

| N2200:SEBS | 100:0 | 75:25 | 50:50 | 30:70 | 10:90 | 5:95 |
|---|---|---|---|---|---|---|
| Mobility | 0.10±0.01 | 0.09±0.02 | 0.12±0.01 | 0.13±0.02 | 0.08±0.01 | 0.05±0.02 |
| $V_{th}$ (V) | 6.5±1.1 | 5.15±0.8 | 6.02±0.7 | 5.34±1.2 | 5.09±1.2 | 5.25±0.9 |
| $I_{on}/I_{off}$ | $>10^3$ | $>10^4$ | $>10^3$ | $>10^4$ | $>10^4$ | $>10^4$ |

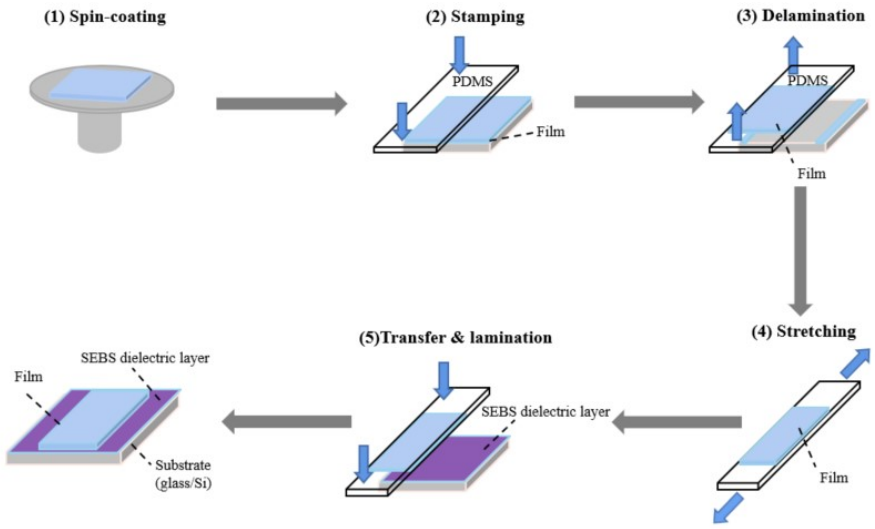


**Figure S2.** Experimental procedure of the FOE method used to prepare the N2200 neat and N2200/SEBS thin films under strain.

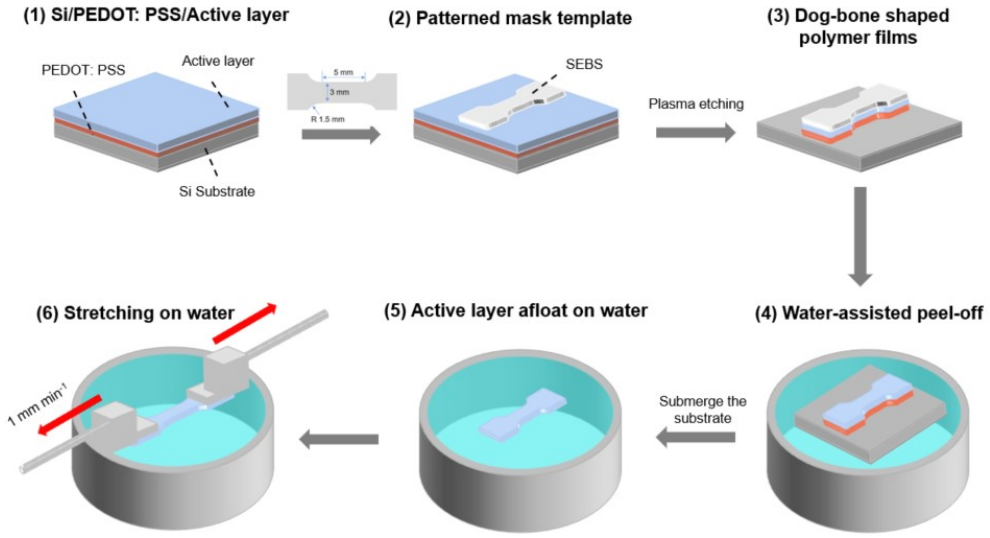


**Figure S3.** Experimental procedure of the FOW method used to obtain the stress–strain curves of the N2200 neat and N2200/SEBS blend films.

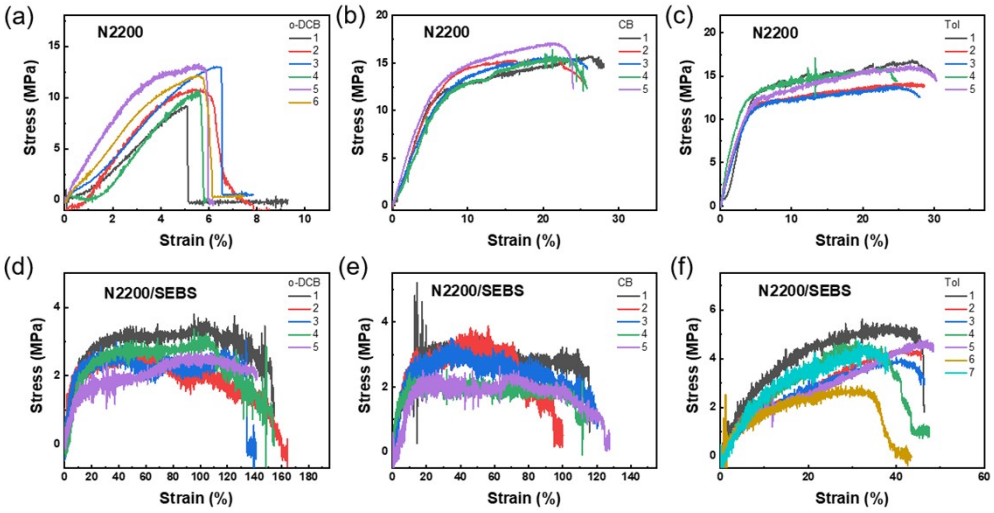


**Figure S4.** All the stress-strain curves of neat N2200 and N2200/SEBS films processed by *o*-DCB, CB, and Tol solvents to provide statistically averaged mechanical properties.

**Table S2.** Corresponding crack onset strain, elastic modulus, and strain at fracture of neat N2200 and N2200/SEBS blend films prepared by *o*-DCB, CB, and Tol.

| Experiment method | Mechanical parameter | N2200 | | | N2200/SEBS | | |
|---|---|---|---|---|---|---|---|
| | | *o*-DCB | CB | Tol | *o*-DCB | CB | Tol |
| FOE | COS (%) | 15~20 | 40~45 | 45~50 | >150 | >150 | 60~65 |
| FOW | Elastic Modulus (MPa) | 306±45 | 277±38 | 282±62 | 22.2±4.5 | 22.6±4.2 | 31.4±3.7 |
| | COS (%) | 6.1±2.2 | 25.0±6.1 | 27.2±2.0 | 153±17 | 118±16 | 42.3±10.5 |

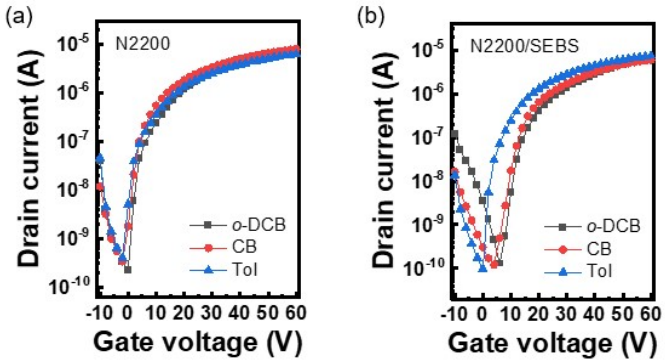


**Figure S5**. Transfer curves ($V_D$ =60 V) of the (a) neat N2200 and (b) N2200/SEBS blend films prepared by different solvents.

**Table S3**. Corresponding mobility of influence of the solvents on the original mobility and the stretchability of neat N2200 and N2200/SEBS blend films.

| Film | Dielectric layer | $\mu$ ($cm^2 V^{-1} s^{-1}$) | | | $V_{th}$ (V) | $I_{on}/I_{off}$ |
|---|---|---|---|---|---|---|
| | | *o*-DCB | CB | Tol | | |
| N2200 | $SiO_2$ | 0.11±0.01 | 0.10±0.03 | 0.12±0.01 | 4.2±1.8 | $>10^4$ |
| N2200/SEBS | | 0.13±0.02 | 0.16±0.03 | 0.19±0.02 | 8.2±3.7 | $>10^4$ |

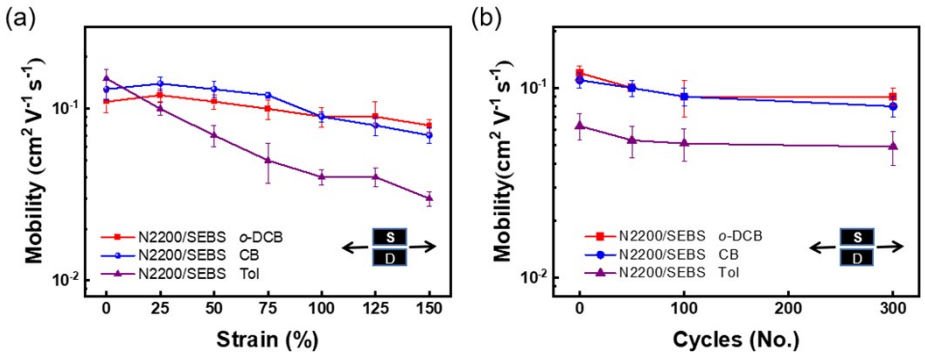


**Figure S6.** (a) Evolution of the mobility of the N2200/SEBS blend films under strain perpendicular to the charge transport direction. (b) Change of the mobility of blend films during repeated stretching cycles at 100% strain perpendicular to the charge transport direction.

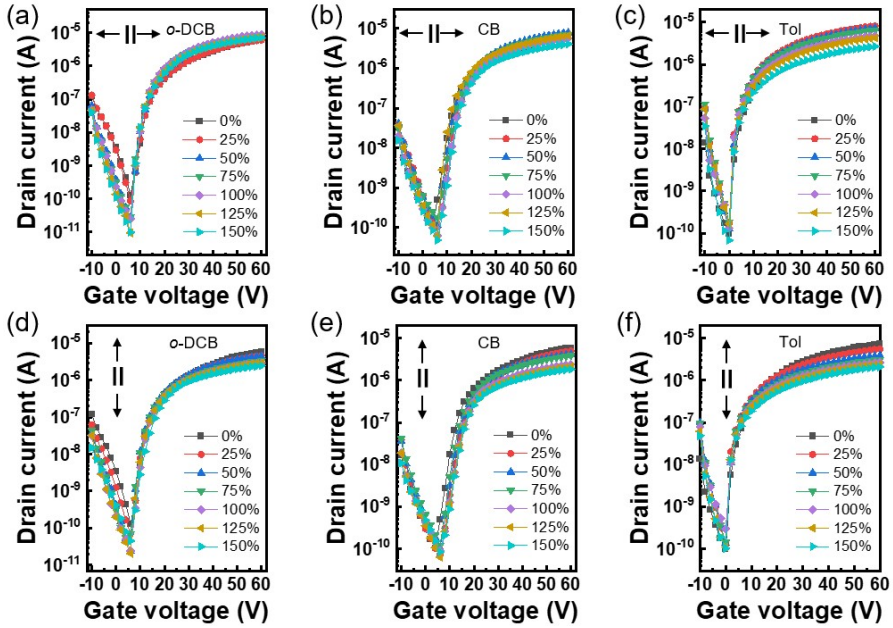


**Figure S7.** Transfer curves ($V_D$ =60 V) of N2200/SEBS blend films prepared by *o*-DCB, CB, and Tol solvents under the stretching up to 150% strain parallel and perpendicular to the charge transport direction.

**Table S4**. Corresponding mobility of the blend films prepared by different solvents under the stretching up to 150% strain parallel and perpendicular to the charge transport direction.

| Strain | *o*-DCB | | CB | | Tol | | $V_{th}$ (V) | $I_{on}/I_{off}$ |
|---|---|---|---|---|---|---|---|---|
| | $\mu_{//}$ ($cm^2 V^{-1} s^{-1}$) | $\mu_{\perp}$ ($cm^2 V^{-1} s^{-1}$) | $\mu_{//}$ ($cm^2 V^{-1} s^{-1}$) | $\mu_{\perp}$ ($cm^2 V^{-1} s^{-1}$) | $\mu_{//}$ ($cm^2 V^{-1} s^{-1}$) | $\mu_{\perp}$ ($cm^2 V^{-1} s^{-1}$) | | |
| 0 | 0.11±0.01 | | 0.13±0.02 | | 0.15±0.02 | | | |
| 25 | 0.15±0.02 | 0.12±0.01 | 0.19±0.02 | 0.14±0.02 | 0.16±0.01 | 0.10±0.01 | | |
| 50 | 0.21±0.02 | 0.11±0.01 | 0.25±0.04 | 0.13±0.02 | 0.13±0.03 | 0.07±0.01 | | |
| 75 | 0.24±0.03 | 0.10±0.01 | 0.24±0.02 | 0.12±0.01 | 0.11±0.02 | 0.05±0.01 | 9.7±3.2 | $>10^4$ |
| 100 | 0.26±0.02 | 0.09±0.01 | 0.20±0.03 | 0.09±0.01 | 0.08±0.01 | 0.04±0.02 | | |
| 125 | 0.23±0.01 | 0.09±0.02 | 0.19±0.01 | 0.08±0.01 | 0.07±0.02 | 0.04±0.01 | | |
| 150 | 0.22±0.01 | 0.08±0.01 | 0.16±0.01 | 0.07±0.02 | 0.04±0.01 | 0.03±0.01 | | |

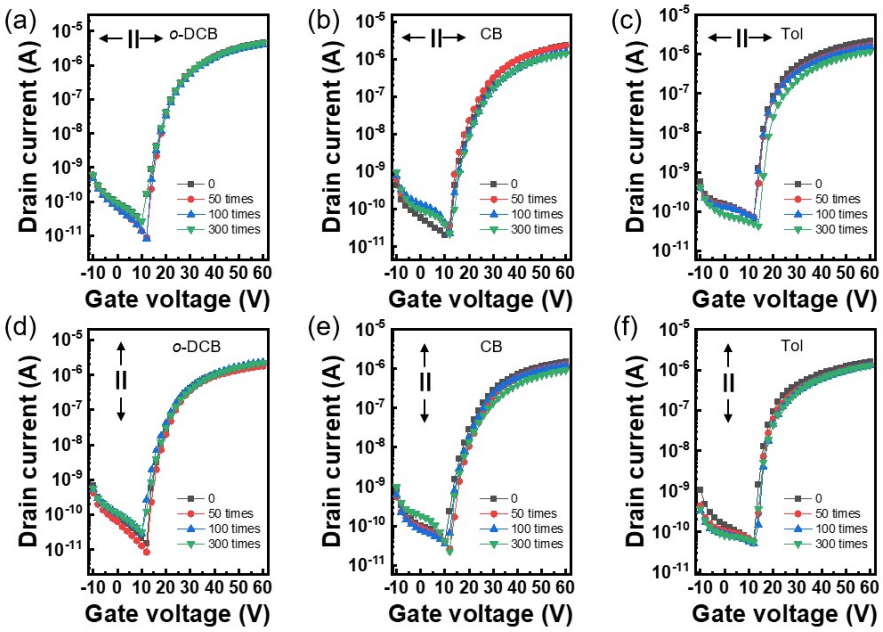


**Figure S8**. Transfer curves ($V_D$ =60 V) of N2200/SEBS blend films prepared by *o*-DCB, CB, and Tol solvents during repeated stretching cycles at 100% strain parallel and perpendicular to the charge transport direction.

**Table S5.** Corresponding mobility of the N2200/SEBS blend films prepared by *o*-DCB, CB, and Tol during repeated stretching cycles at 100% strain parallel and perpendicular to the charge transport direction.

| Repeated cycles | *o*-DCB | | CB | | Tol | | $V_{th}$ (V) | $I_{on}/I_{off}$ |
|---|---|---|---|---|---|---|---|---|
| | $\mu_{//}$ ($cm^2 V^{-1} s^{-1}$) | $\mu_{\perp}$ ($cm^2 V^{-1} s^{-1}$) | $\mu_{//}$ ($cm^2 V^{-1} s^{-1}$) | $\mu_{\perp}$ ($cm^2 V^{-1} s^{-1}$) | $\mu_{//}$ ($cm^2 V^{-1} s^{-1}$) | $\mu_{\perp}$ ($cm^2 V^{-1} s^{-1}$) | | |
| 0 | 0.24±0.03 | 0.12±0.01 | 0.21±0.02 | 0.11±0.01 | 0.10±0.01 | 0.06±0.01 | 14.3±2.5 | $>10^4$ |
| 50 | 0.23±0.04 | 0.10±0.01 | 0.19±0.01 | 0.10±0.01 | 0.08±0.02 | 0.05±0.01 | | |
| 100 | 0.23±0.02 | 0.09±0.02 | 0.14±0.01 | 0.09±0.01 | 0.07±0.01 | 0.05±0.01 | | |
| 300 | 0.22±0.03 | 0.09±0.01 | 0.13±0.02 | 0.09±0.01 | 0.06±0.01 | 0.05±0.01 | | |

**Table S6**. GIXRD parameters of neat N2200 films processed by *o*-DCB, CB, and Tol.

| Solvent | Peak | Out-of-plane | | | | In-plane | | | |
|---|---|---|---|---|---|---|---|---|---|
| | | Peak position (°) | d-spacing (Å) | FWHM (°) | CCL (Å) | Peak position (°) | d-spacing (Å) | FWHM (°) | CCL (Å) |
| *o*-DCB | (100) | 3.80 | 23.22 | - | | 3.46 | 25.50 | 0.51 | 76.99 |
| | (001) | - | - | - | | 6.38 | - | - | - |
| | (010) | 22.64 | 3.92 | 4.94 | 7.96 | - | - | - | - |
| CB | (100) | - | - | - | | 3.46 | 25.50 | 0.50 | 78.53 |
| | (001) | - | - | - | | 6.40 | - | - | |
| | (010) | 22.65 | 3.92 | 4.33 | 9.07 | - | - | - | - |
| Tol | (100) | 3.85 | 22.92 | - | | 3.44 | 25.65 | 0.49 | 80.13 |
| | (001) | - | - | - | | 6.40 | - | - | - |
| | (010) | 22.62 | 3.93 | 3.79 | 10.37 | - | - | - | - |

**Table S7**. GIXRD parameters of the N2200/SEBS blend films processed by *o*-DCB, CB, and Tol.

| Solvent | Peak | Out-of-plane | | | | In-plane | | | |
|---|---|---|---|---|---|---|---|---|---|
| | | Peak position (°) | d-spacing (Å) | FWHM (°) | CCL (Å) | Peak position (°) | d-spacing (Å) | FWHM (°) | CCL (Å) |
| *o*-DCB | (100) | 3.51 | 25.14 | 0.57 | 68.88 | 3.43 | 25.73 | 0.52 | 75.51 |
| | (200) | 7.02 | 25.14 | - | - | - | - | - | - |
| | (001) | - | - | - | - | 6.37 | 13.86 | - | - |
| | (010) | 20.78 | 4.27 | 5.81 | 6.77 | 20.96 | 4.23 | - | - |
| CB | (100) | 3.48 | 25.36 | 0.63 | 62.32 | 3.41 | 25.88 | 0.50 | 78.53 |
| | (200) | 6.96 | 25.36 | - | - | - | - | - | - |
| | (001) | - | - | - | - | 6.39 | 13.81 | - | - |
| | (010) | 20.80 | 4.26 | 6.37 | 6.17 | 21.16 | 4.19 | - | - |
| Tol | (100) | 3.54 | 24.93 | 0.54 | 72.71 | 3.35 | 25.34 | 0.44 | 89.24 |
| | (200) | 7.08 | 24.93 | - | - | - | - | - | - |
| | (001) | - | - | - | - | 6.38 | 13.83 | - | - |
| | (010) | 20.80 | 4.26 | 6.36 | 6.18 | 20.82 | 4.26 | - | - |

**Table S8.** The detailed dispersion component $\delta_D$, polar component $\delta_P$, and hydrogen-bonding component $\delta_H$ of the HSP for N2200, SEBS and solvents.

| Solvent | $\delta_D$ (MPa$^{1/2}$) | $\delta_P$ (MPa$^{1/2}$) | $\delta_H$ (MPa$^{1/2}$) |
|---|---|---|---|
| *o*-DCB | 19.2 | 6.3 | 3.3 |
| CB | 19.0 | 4.3 | 2.0 |
| Tol | 18.0 | 1.4 | 2.0 |
| SEBS | 17.5 | 0.3 | 0 |
| N2200 | 19.9 | 1.4 | 3.1 |
| Side chain | 15.9 | 0.1 | 0.1 |
| Backbone | 23.0 | 5.1 | 7.1 |

**Table S9**. The solubility distance ($R_a$) of solvents to the side chain, backbone, N2200 molecule and SEBS calculated using the Yamamoto-Molecular Break (Y-MB) option in HSPiP software.

| Solvent | N2200 | | SEBS | |
|---|---|---|---|---|
| | $R_{a(b)}$ (MPa$^{1/2}$) | $R_{a(s)}$ (MPa$^{1/2}$) | $R_a$ (MPa$^{1/2}$) | $R_a$ (MPa$^{1/2}$) |
| *o*-DCB | 8.58 | 9.60 | 5.04 | 7.65 |
| CB | 9.52 | 7.72 | 3.50 | 5.39 |
| Tol | 11.82 | 4.79 | 3.76 | 2.49 |

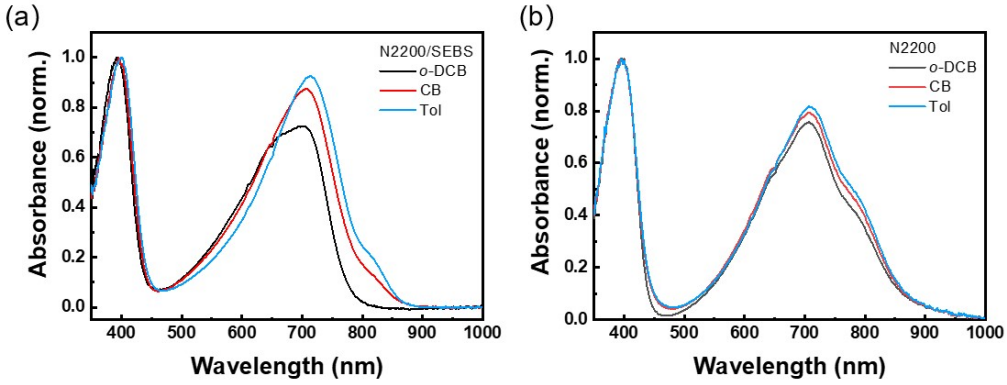


**Figure S9.** (a) UV-vis absorption spectra of N2200 solutions in *o*-DCB, CB, and Tol with the concentration of 0.1 mg mL$^{-1}$. (b) UV-vis absorption spectra of neat N2200 films prepared by *o*-DCB, CB, and Tol. The absorption spectra are normalized at ~400 nm.

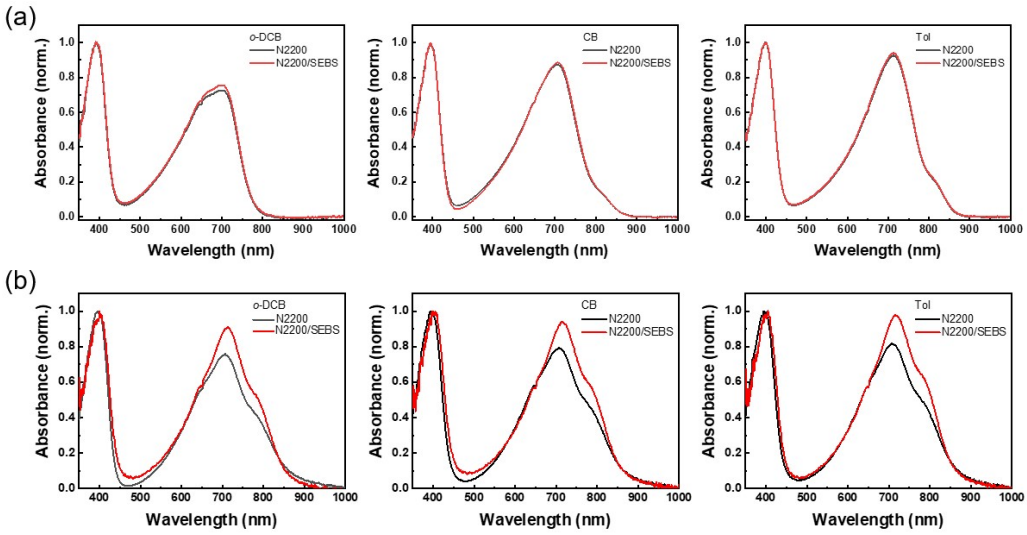


**Figure S10**. UV-vis absorbance spectra of (a) solutions and (b) films of neat N2200 and N2200/SEBS blends processed by different solvents.

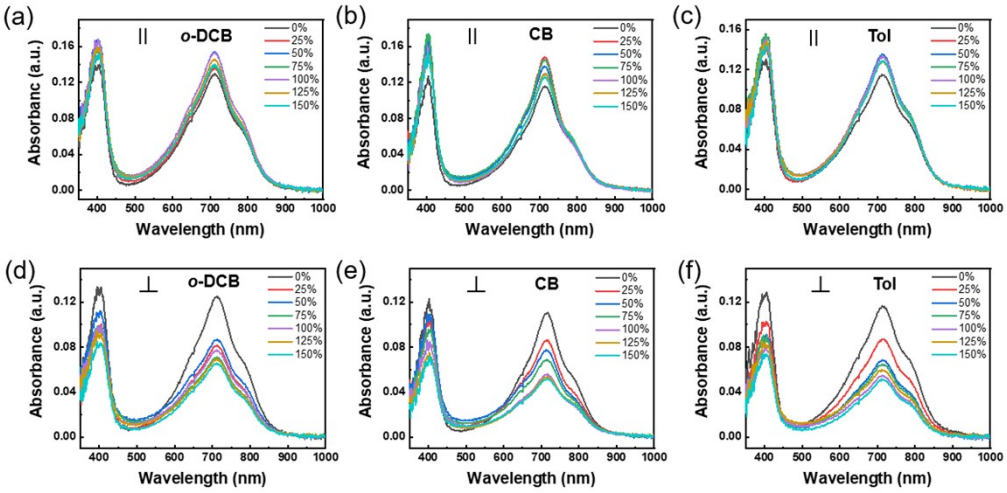


**Figure S11.** Polarized UV-vis spectra of stretched N2200/SEBS blend films prepared by (a, d) *o*-DCB, (b, e) CB, and (c, f) Tol, with the polarization direction of incident beam (a, b, c) parallel and (d, e, f) perpendicular to the stretching direction.

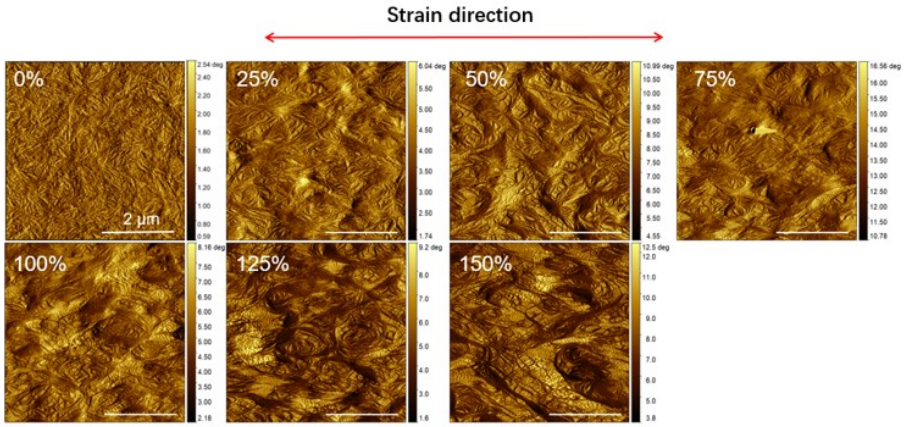


**Figure S12.** AFM phase images of N2200/SEBS blend films prepared by *o*-DCB at different strains.

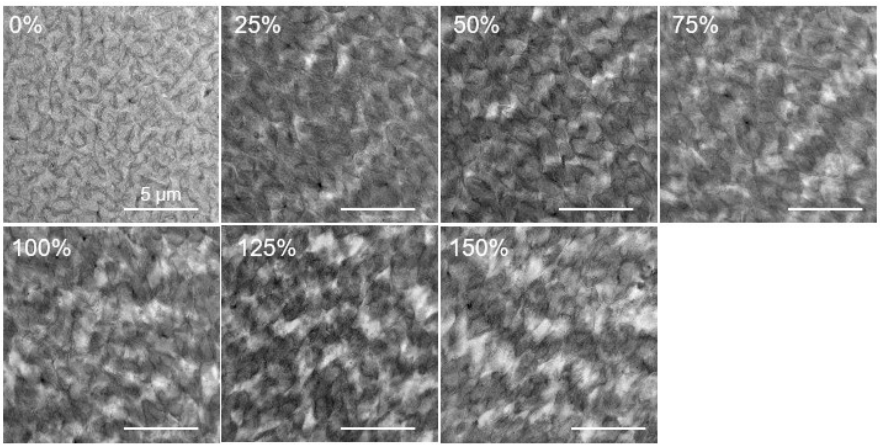


**Figure S13.** TEM images of N2200/SEBS blend films prepared by *o*-DCB at different strains.

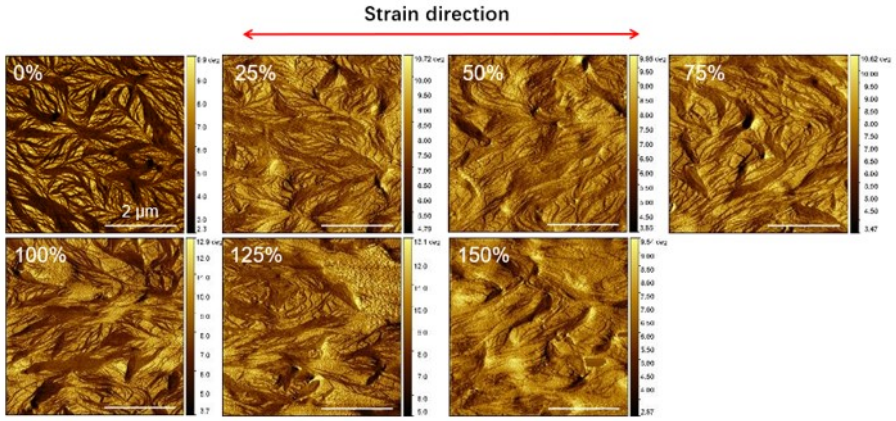


**Figure S14.** AFM phase images of N2200/SEBS blend films prepared by CB at different strains.

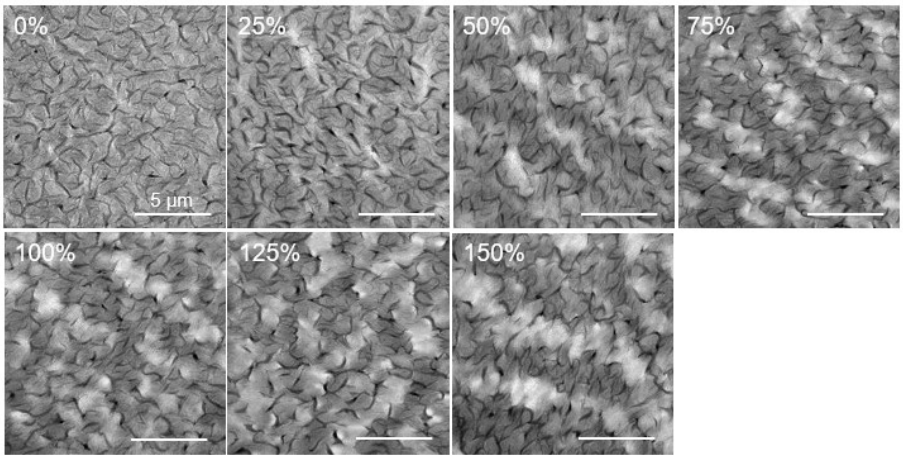


**Figure S15.** TEM images of N2200/SEBS blend films prepared by CB at different strains.

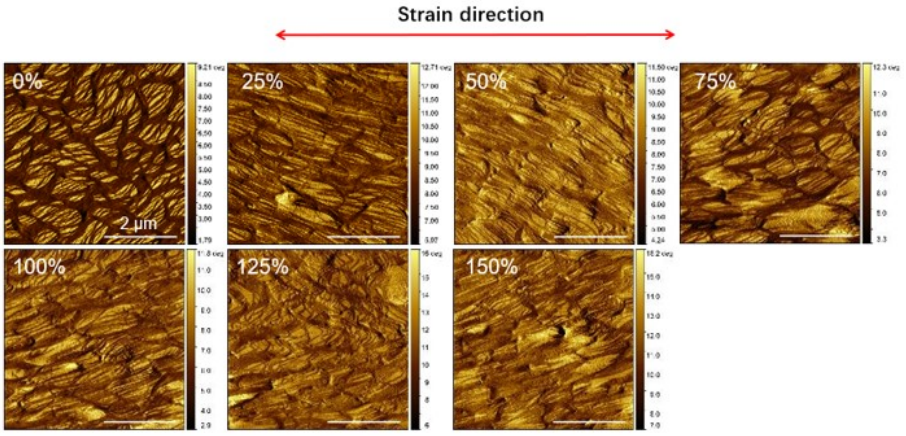


**Figure S16.** AFM phase images of N2200/SEBS blend films prepared by Tol at different strains.

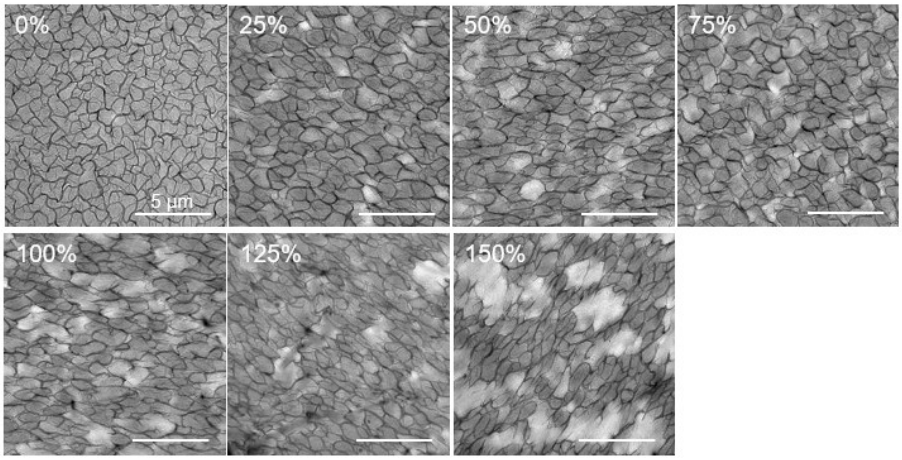


**Figure S17.** TEM images of N2200/SEBS blend films prepared by Tol at different strains.

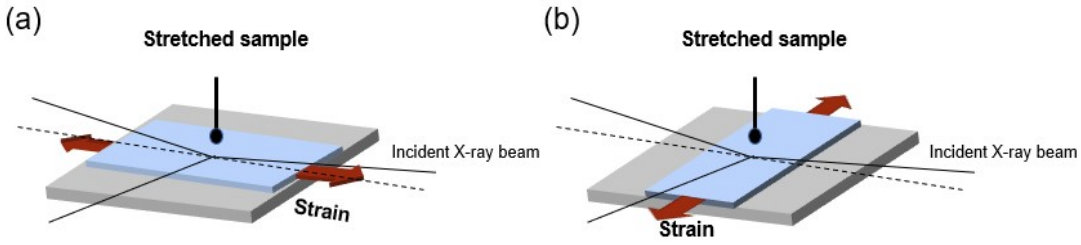


**Figure S18.** Schematic illustration of the strain-dependent GIXRD measurement for X-ray (a) parallel and (b) perpendicular to the strain direction

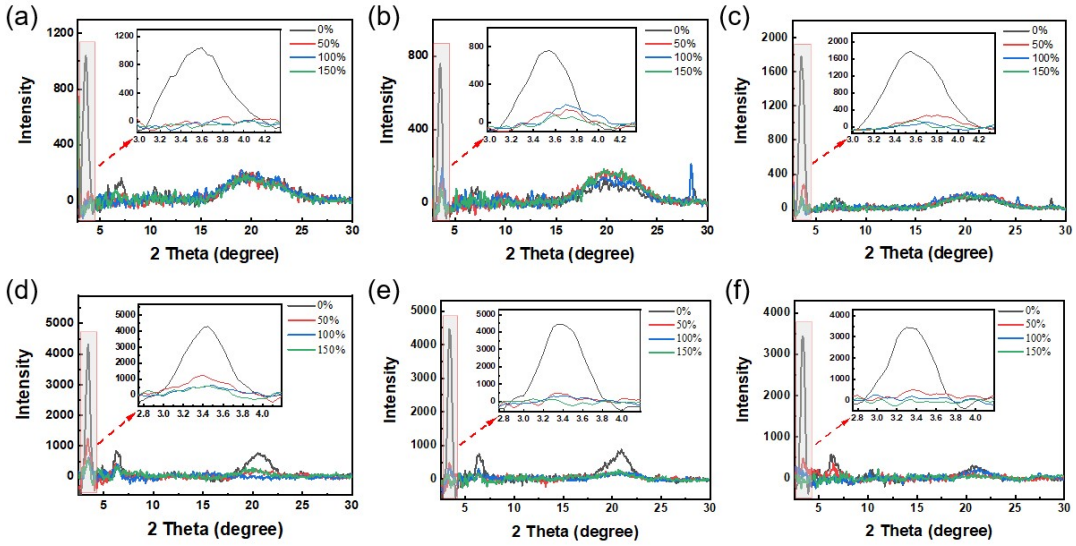


**Figure S19.** GIXRD profiles of N2200/SEBS blend film prepared by (a, d) *o*-DCB, (b, e) CB and (c, f) Tol with X-ray perpendicular to strain direction: (a, b, c) 1D out-of-plane; (d, e, f) 1D in-plane.

**Table S10**. GIXRD parameters of the *o*-DCB-processed blend films with/without strains.

| Strain | Peak | Out-of-plane | | | | In-plane | | | |
|---|---|---|---|---|---|---|---|---|---|
| | | Peak position (°) | d-spacing (Å) | FWHM (°) | CCL (Å) | Peak position (°) | d-spacing (Å) | FWHM (°) | CCL (Å) |
| 0% | (100) | 3.51 | 25.14 | 0.55 | 71.39 | 3.43 | 25.73 | 0.48 | 81.80 |
| | (200) | 7.02 | 25.14 | - | - | - | - | - | - |
| | (001) | - | - | - | - | 6.37 | 13.86 | - | - |
| | (010) | 20.78 | - | 6.82 | 5.77 | 20.96 | 4.23 | 2.60 | 15.11 |
| 50% | (100) | 3.82 | 23.10 | 0.57 | 68.88 | 3.42 | 25.80 | 0.49 | 80.13 |
| | (010) | 20.69 | 4.28 | 5.68 | 6.92 | 20.46 | 4.33 | 3.91 | 10.05 |
| 100% | (100) | 3.78 | 23.35 | 0.61 | 64.37 | 3.42 | 25.80 | 0.50 | 78.53 |
| | (010) | 20.69 | 4.28 | 6.67 | 5.90 | - | - | 2.91 | 13.50 |
| 150% | (100) | 3.76 | 23.47 | 0.69 | 56.91 | 3.44 | 25.65 | 0.45 | 87.26 |
| | (010) | 20.69 | 4.28 | 5.86 | 6.71 | - | - | 3.27 | 12.01 |

**Table S11**. GIXRD parameters of the CB-processed blend films with/without strains.

| Strain | Peak | Out-of-plane | | | | In-plane | | | |
|---|---|---|---|---|---|---|---|---|---|
| | | Peak position (°) | d-spacing (Å) | FWHM (°) | CCL (Å) | Peak position (°) | d-spacing (Å) | FWHM (°) | CCL (Å) |
| 0% | (100) | 3.48 | 25.36 | 0.44 | 89.24 | 3.41 | 25.88 | 0.47 | 83.54 |
| | (200) | 6.96 | 25.36 | - | - | - | - | - | - |
| | (001) | - | - | - | - | 6.39 | 13.81 | - | - |
| | (010) | 20.80 | 4.26 | 5.81 | 6.77 | 21.16 | 4.19 | 2.64 | 14.87 |
| 50% | (100) | 3.56 | 24.79 | 0.49 | 80.13 | 3.47 | 25.43 | 0.50 | 78.53 |
| | (010) | 20.80 | 4.26 | 6.25 | 6.29 | - | - | - | - |
| 100% | (100) | 3.60 | 24.51 | 0.38 | 103.3 | 3.44 | 25.65 | 0.48 | 81.80 |
| | (010) | 20.80 | 4.26 | 5.92 | 6.64 | - | - | - | - |
| 150% | (100) | 3.58 | 24.65 | 0.47 | 83.54 | 3.45 | 25.58 | 0.44 | 89.24 |
| | (010) | 20.80 | 4.26 | 6.08 | 6.47 | - | - | 4.32 | 9.10 |

**Table S12**. GIXRD parameters of the Tol-processed blend films with/without strains.

| Strain | Peak | Out-of-plane | | | | In-plane | | | |
|---|---|---|---|---|---|---|---|---|---|
| | | Peak position (°) | d-spacing (Å) | FWHM (°) | CCL (Å) | Peak position (°) | d-spacing (Å) | FWHM (°) | CCL (Å) |
| 0% | (100) | 3.54 | 24.93 | 0.57 | 68.89 | 3.35 | 26.34 | 0.48 | 81.80 |
| | (200) | 7.08 | 24.93 | - | - | - | - | - | - |
| | (001) | - | - | - | - | 6.38 | 13.83 | - | - |
| | (010) | 20.80 | 4.26 | 6.36 | 6.19 | 20.82 | 4.26 | - | - |
| 50% | (100) | 3.68 | 23.98 | 0.59 | 66.55 | 3.38 | 26.11 | 0.53 | 74.08 |
| | (010) | 20.80 | 4.26 | 6.10 | 6.45 | 20.82 | 4.26 | - | - |
| 100% | (100) | 3.67 | 24.04 | 0.50 | 78.53 | 3.41 | 25.88 | 0.51 | 76.99 |
| | (010) | 20.76 | 4.27 | 5.79 | 6.79 | 20.82 | 4.26 | - | - |
| 150% | (100) | 3.65 | 24.18 | 0.53 | 74.08 | 3.40 | 25.96 | 0.50 | 78.53 |
| | (010) | 20.80 | 4.26 | 5.98 | 6.58 | 20.82 | 4.26 | - | - |